

Allanpringite, $\text{Fe}_3(\text{PO}_4)_2(\text{OH})_3 \cdot 5\text{H}_2\text{O}$, a new ferric iron phosphate from Germany, and its close relation to wavellite

UWE KOLITSCH^{1*}, HEINZ-JÜRGEN BERNHARDT², CHRISTIAN L. LENGAUER¹, GÜNTER BLASS³
and EKKEHART TILLMANN¹

¹Institut für Mineralogie und Kristallographie, Geozentrum, Universität Wien, Althanstr. 14, 1090 Wien, Austria

*Corresponding author, e-mail: uwe.kolitsch@univie.ac.at

²Ruhr-Universität Bochum, Zentrale Elektronen-Mikrosonde, Universitätsstr. 150, 44801 Bochum, Germany

³Merzbachstr. 6, 52249 Eschweiler, Germany

Abstract: Allanpringite is a new ferric iron phosphate with the ideal formula $\text{Fe}_3(\text{PO}_4)_2(\text{OH})_3 \cdot 5\text{H}_2\text{O}$, and is closely related to wavellite, $\text{Al}_3(\text{PO}_4)_2(\text{OH})_3 \cdot 5\text{H}_2\text{O}$. Type locality is the dump of the abandoned Grube Mark near Essershausen, ca. 5 km SE of Weilburg/Lahn, Taunus, Hesse, Germany. The mineral occurs as pale brown-yellow, [010] acicular, invariably twinned (by non-merohedry) crystals which are always intergrown to form bundles of subparallel individuals. The maximum length of crystals is ca. 1.5 mm (usually much smaller); bundles can reach up to about 2 mm. The mineral is associated with beraunite (reddish “oxiberaunite” variety), cacoxenite, strengite and cryptomelane. Allanpringite is translucent to transparent, its streak is white with a pale yellowish tint, and it has a vitreous lustre. It shows a perfect cleavage parallel to the morphological elongation and one good cleavage parallel to {010}. It is brittle and has an uneven fracture, a Mohs hardness of ~3, and $D(\text{meas.}) = 2.54(2)$ g/cm³, $D(\text{calc.}) = 2.583$ g/cm³ (for empirical formula). Optically, it is biaxial positive, with $\alpha = 1.662(5)$, $\beta = 1.675(5)$, $\gamma = 1.747(5)$, $2V\gamma(\text{calc.}) = 48^\circ$; pleochroism is strong: X colourless, Y colourless, Z dark yellow; absorption $Z \gg X \sim Y$; orientation $XYZ = **b$ (pseudo-orthorhombic); no visible dispersion. Electron microprobe analysis yielded (wt. %): Fe_2O_3 47.84, Al_2O_3 0.34, Mn_2O_3 0.04; CuO 0.08, P_2O_5 28.56, F 0.02, $\text{H}_2\text{O}_{\text{calc}}$ 23.49, less $\text{O} \equiv \text{F}$ 0.01, total 100.36. The empirical formula is $(\text{Fe}_{2.98}\text{Al}_{0.03})(\text{PO}_4)_2(\text{OH}_{3.02}\text{F}_{0.01}) \cdot 4.97\text{H}_2\text{O}$, based on 16 O atoms.

Allanpringite is monoclinic, space group $P2_1/n$, with $a = 9.777(3)$, $b = 7.358(2)$, $c = 17.830(5)$ Å, $\beta = 92.19(4)^\circ$, $V = 1281.7(6)$ Å³ (single-crystal data) and $Z = 4$. Strongest lines in the X-ray powder diffraction pattern are [d (Å), I , hkl]: 8.90 (100) (002), 8.41 (60) (10-1, 101), 5.870 (50) (110), 3.600 (50) (021, 02-1), 3.231 (80) (204, 12-2). The crystal structure has been determined using single-crystal X-ray diffraction data (MoK α radiation, CCD area detector) obtained from a twinned fragment ($R(F) = 13.3\%$). The structure of allanpringite is a monoclinically distorted, pseudo-orthorhombic variant of the orthorhombic structure of its Al-analogue wavellite, $\text{Al}_3(\text{PO}_4)_2(\text{OH},\text{F})_3 \cdot 5\text{H}_2\text{O}$. Chains of corner-sharing, distorted $\text{Fe}(\text{O},\text{OH},\text{H}_2\text{O})_6$ octahedra parallel to [010] are corner-linked by PO_4 tetrahedra. Channels, also parallel to [010], host a positionally split water molecule. Average Fe-O distances of the three non-equivalent Fe atoms range between 2.014 and 2.021 Å. Single-crystal laser-Raman spectroscopy confirms an overall weak hydrogen bonding scheme. The structure of allanpringite is also related to those of kingite and mitryaevaite. The amorphous santabarbarite has a chemical formula basically identical to that of allanpringite. The name honours Dr. Allan Pring, eminent Australian mineralogist.

Key-words: allanpringite, new mineral, ferric iron phosphate, crystal structure, wavellite.

Introduction

In 1999, samples of an unidentified secondary phosphate mineral, forming pale brown-yellow bundles of small acicular crystals, were collected by Mr. Michael Legner of Villmar, Germany, on the dump of a small old iron mine in the Taunus area, Germany, and were subsequently submitted to one of the authors (G. B.). Preliminary chemical analyses showed that the new mineral was an Fe-phosphate containing minor Al. A powder X-ray diffraction pattern could not be matched to any known mineral or synthetic compound.

Preliminary single-crystal studies failed because all crystals were invariably twinned by non-merohedry and generally of poor quality and small size. A complete characterisation of the mineral was only possible after a crystal fragment was finally found that was suitable for a single-crystal structure determination. A preliminary characterisation of the new mineral was given by Kolitsch *et al.* (2004). The mineral and its name were unanimously approved by the Commission on New Minerals and Mineral Names, IMA (no. 2004-050). The name is in honour of Dr. Allan Pring, Australian mineralogist, in recognition of his numerous contributions

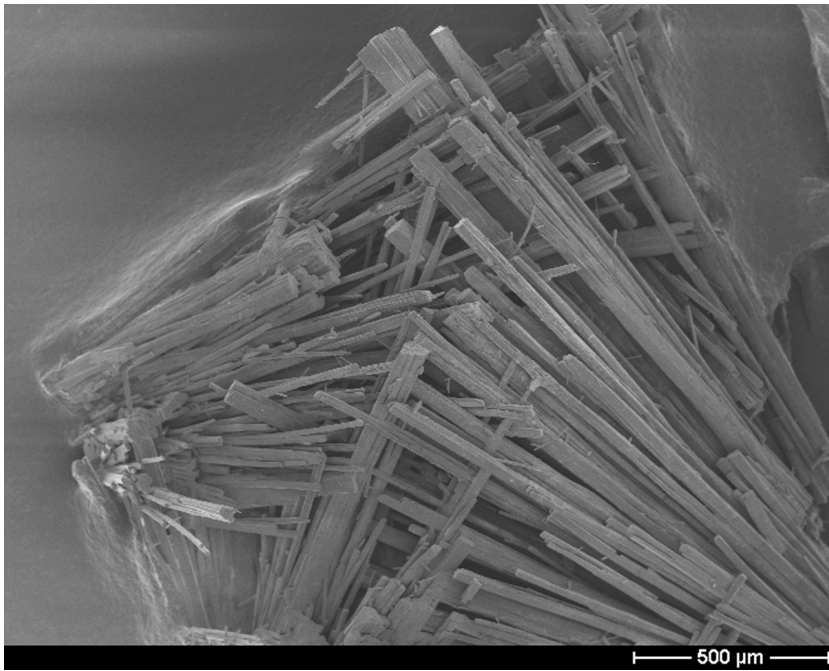


Figure 1: SEM micrograph of twinned (by non-merohedry) prismatic [010] crystals of allanpringite. The tiny needles covering some parts of the prisms are cacoxenite crystals.

to the “mineralogical rainforest” (especially on phosphates, arsenates and sulfosalts). The type specimen is preserved in the collection of the Natural History Museum, Vienna, Austria.

The present work is part of studies devoted to the crystal chemistry of several complex fibrous iron phosphate minerals (Kolitsch, 1999, 2001, 2004).

Occurrence and paragenesis

Allanpringite was found on the dump of the abandoned Grube Mark near Essershausen, ca. 5 km SE of Weilburg/Lahn, Taunus, Hesse, Germany. The Grube Mark is a small old iron mine with “limonite” (predominantly consisting of botryoidal goethite) as the main ore. The deposit was formed during Tertiary weathering processes (Bläß, 2002), and the ore was mined from 1828 to 1914, and also briefly in the 1940s. It consisted of a “limonite” layer with a thickness of 1–4 m, and an extension of 300 m. Toward the depth of the deposit, fine-grained siderite was sometimes encountered. The ore was characterised by small contents of Mn (1–3%) and P (1%). Rarely, small nests of phosphorite ore and secondary phosphates were encountered.

Allanpringite has only been found on the mentioned dump, but not on dumps of any of the other, adjacent small iron mines (M. Legner, pers. comm., 2004). The new mineral, for which a brief preliminary description as a “new iron-aluminium phosphate” was given by Bläß (2002), is associated with beraunite (reddish “oxiberaunite” variety; fresh crystals up to 1 mm), cacoxenite (small sprays, hemispheres and felty coatings), strengite (small white opaque globules) and cryptomelane (massive, earthy). The type locality is also known for several other secondary phosphates (Bläß, 2002): chalcosiderite, dufrenite, natrodufrenite(?), kidwel-

lite, phosphosiderite, planerite, pseudomalachite, rockbridgite, strengite, tinctite, turquoise, vantasselite and wavellite; non-phosphate species identified are jarosite, cryptomelane, pyrolusite, goethite, hematite and quartz (Bläß, 2002). As judged from its paragenesis, allanpringite is a supergene (or possibly a very-low-temperature hydrothermal) mineral. It has formed contemporaneously with, or later than, beraunite, and is sometimes overgrown by cacoxenite. However, cacoxenite can also form the basis of beraunite and allanpringite. The iron in all accompanying phosphates is trivalent, indicating oxidising conditions of formation also for allanpringite.

Appearance and physical properties

Allanpringite forms pale brown-yellow, translucent to transparent, [010] acicular, twinned crystals which are always intergrown to form bundles of subparallel individuals (Fig. 1). The maximum length of crystals is ca. 1.5 mm (usually much smaller); bundles can reach up to about 2 mm. The only clearly recognisable crystal form is {010} (perpendicular to the morphological elongation), although the crystal termination sometimes is also rounded and may be composed of several different {*hkl*} forms. Due to twinning and pervasive subparallel intergrowth, no prism forms could be identified without ambiguity. The twinning is by non-merohedry and parallel to the morphological elongation, as shown by single-crystal studies; it is not visible under the polarising microscope.

Allanpringite is translucent to transparent, its streak is white with a pale yellowish tint, and it has a vitreous lustre. It shows a perfect cleavage parallel to the morphological elongation (probably parallel to {101}) and a good cleavage parallel to {010}. It is brittle and has an uneven fracture, a

Table 1. Electron microprobe analysis of allanpringite.

	wt. %	Range	Stand. Dev.	wt. % (ideal)
Fe ₂ O ₃	47.84	45.67 – 49.34	1.05	48.04
Al ₂ O ₃	0.34	0.06 – 1.67	0.36	
Mn ₂ O ₃	0.04	0.00 – 0.12	0.04	
CuO	0.08	0.00 – 0.49	0.14	
P ₂ O ₅	28.56	27.57 – 29.54	0.60	28.47
F	0.02	0.00 – 0.08	0.02	
H ₂ O*	23.49			23.49
O≡F	-0.01			
Total	100.36			100.00

Notes: Number of analyses = 7. Probe standards: synth. andradite (Fe), synth. pyrope (Al), synth. spessartine (Mn), synth. CuO (Cu), synth. AlPO₄ (P), analysed topaz (F). The empirical formula is (Fe_{2.98}Al_{0.03})(PO₄)₂(OH_{3.02}F_{0.01})·4.97H₂O (based on 16 oxygen atoms).

* calculated from structure solution.

Mohs hardness of ~3, and $D(\text{meas.}) = 2.54(2) \text{ g/cm}^3$, $D(\text{calc.}) = 2.583 \text{ g/cm}^3$ (for empirical formula). Optically, it is biaxial positive, with $\alpha = 1.662(5)$, $\beta = 1.675(5)$, $\gamma = 1.747(5)$, $2V\gamma(\text{calc.}) = 48^\circ$; pleochroism is strong: X colourless, Y colourless, Z dark yellow; absorption $Z \gg X \sim Y$; orientation $XYZ = **b$ (pseudo-orthorhombic); no visible dispersion.

Chemical composition

Quantitative electron microprobe analysis (CAMECA SX50) was used to determine the chemical composition of allanpringite. Because the mineral showed a slight tendency to dehydrate under the electron beam, measurement parameters were modified accordingly (acceleration voltage 15 kV, beam current 10 nA, beam diameter ca. 5 μm , counting time 20 s). Additionally, the polished grains were moved under the electron beam. A slow and minor dehydration could not be prevented, however. Non-oxygen elements detected were Fe, P, Al (minor), Mn (traces) and F (traces). A wavelength-dispersive scan indicated the absence of any other elements with $Z > 8$. As there was insufficient amount of material for a direct determination of the water content, it was calculated from the crystal-structure solution. Table 1 summarises the analytical data which led to the empirical formula (Fe_{2.98}Al_{0.03})(PO₄)₂(OH_{3.02}F_{0.01})·4.97H₂O, based on 16 O atoms, and are in good agreement with the results of the crystal-structure determination (see below). In the core parts of the crystals, the Al contents were somewhat higher than in the outer parts. A slight variability of the Al contents was also observed during additional SEM-EDS analyses.

X-ray powder diffraction data

X-ray powder diffraction data were obtained with the Gandolfi technique (camera radius 114.59 mm, CuK α radiation, no internal standard). The indexed data, given in Table 2, show good agreement with a theoretical powder pattern cal-

Table 2. X-ray powder diffraction data for allanpringite.

III_{obs}	d_{obs}	III_{calc}^*	d_{calc}^{**}	hkl
100	8.90	100	8.89	002
60	8.41	47	8.71	10-1
		43	8.43	101
50	5.870	42	5.878	110
<10	5.542	5	5.620	11-1
		7	5.545	111
10	5.157	12	5.159	10-3
15	4.982	14	4.990	103
-	-	3	4.959	11-2
30	4.873	36	4.886	200
15	4.445	16	4.451	004
-	-	4	4.227	11-3
-	-	3	4.130	113
-	-	5	4.070	210
-	-	3	3.995	21-1
50	3.600	40	3.603	021,02-1
-	-	4	3.511	114
-	-	3	3.443	120
40	3.357	37	3.354	20-4
		33	3.230	204
80b	3.231	24	3.226	12-2
		28	3.197	122
-	-	3	3.079	11-5
10	2.910	10	2.902	30-3
-	-	5	2.811	303
-	-	3	2.724	21-5
-	-	3	2.700	31-3
<10	2.674	7	2.673	11-6
15	2.627	1	2.626	313
		9	2.625	116
-	-	5	2.610	223
15	2.440	9	2.439	320
<10	2.368	6	2.369	32-2
-	-	6	2.335	322
<10	2.320	3	2.319	410
-	-	5	2.242	225
<10	2.231	2	2.225	008
-	-	4	2.192	230
20	2.177	8	2.177	40-4
-	-	6	2.108	404
-	-	5	2.056	20-8
<10	1.9961	4	1.9970	208
<10	1.9694	4	1.9689	307
<10	1.9107	5	1.9108	32-6
<10	1.8593	6	1.8585	326
<10	1.8399	6	1.8397	040

Notes: Gandolfi camera, diameter 114.59 mm, CuK α , Ni-filter, 16 h; III_{obs} estimated visually. b = broad.

* III_{calc} and hkl indexing based on a theoretical powder pattern calculated from the refined single-crystal structure. ** Derived from the refined unit-cell parameters of the powder data, $a = 9.779(4)$, $b = 7.359(3)$, $c = 17.816(6) \text{ \AA}$, $\beta = 92.16(3)^\circ$.

culated from the refined structure model (see below). The refined unit-cell parameters, with $a = 9.779(4)$, $b = 7.359(3)$, $c = 17.816(6) \text{ \AA}$, $\beta = 92.16(3)^\circ$, $V = 1281.1(6) \text{ \AA}^3$, are basically identical to those obtained by the single-crystal study.

Table 3. Crystal data, data collection information and refinement details for allanpringite.

<i>Crystal data</i>	
Formula	(Fe _{0.92} Al _{0.08}) ₃ (PO ₄) ₂ (OH) ₃ ·5H ₂ O
Space group, <i>Z</i>	<i>P</i> 2 ₁ / <i>n</i> (no. 14), 2
<i>a</i> , <i>b</i> , <i>c</i> (Å)	9.777(3), 7.358(2), 17.830(5)
β (°)	92.19(4)
<i>V</i> (Å ³)	1281.7(6)
<i>F</i> (000), ρ _{calc} (g · cm ⁻³)	983, 2.55
μ (mm ⁻¹)	3.434
Absorption correction	multi-scan*
Crystal dimensions (mm)	0.03 x 0.04 x 0.18**
<i>Data Collection and refinement</i>	
Diffractometer	Nonius KappaCCD system
λ (Mo- <i>K</i> α) (Å), <i>T</i> (K)	0.71073, 293
Crystal-detector dist. (mm)	50
Rotation axis, width (°)	φ, ω, 1
Total no. of frames	1279
Collect. time per degree (s)	250
Collection mode	full sphere
θ range (°)	2 – 30 (used: 4.11 – 27.28)
<i>h</i> , <i>k</i> , <i>l</i> ranges	-12 → 12, -9 → 9, -22 → 22
Total reflections measured	5047
Unique reflections	2645 (<i>R</i> _{int} 4.8 %)
Refinement on	<i>F</i> ²
<i>R</i> 1(<i>F</i>), w <i>R</i> 2 _{all} (<i>F</i> ²)* **	13.3 %, 35.3 %
'Observed' refls.	2045 [<i>F</i> _o > 4σ(<i>F</i> _o)]
Extinct. coefficient	none
No. of refined parameters	116
Goof	1.418
(Δ/σ) _{max}	0.0001
Δρ _{min} , Δρ _{max} (e/Å ³)	-1.2, 4.2

Note: Unit-cell parameters were refined from 3047 recorded reflections.

Scattering factors for neutral atoms were employed in the refinement.

* Otwinowsky & Minor (1997), Otwinowsky *et al.* (2003)

** Dimensions refer to twin.

*** $w = 1/[\sigma^2(F_o^2) + (0.2P)^2 + 0.0P]$; $P = ([\max \text{ of } (0 \text{ or } F_o^2)] + 2F_c^2)/3$

Crystal structure

Structure determination

Single-crystal studies of allanpringite were performed with a Nonius KappaCCD single-crystal X-ray diffractometer equipped with a CCD area detector and a 300 μm diameter capillary-optics collimator to provide increased resolution. All of about ten allanpringite crystals studied (tiny prisms) were twinned by non-merohedry parallel to their morphological elongation. Additionally, a tendency to form subparallel intergrowths was pervasive. Single-crystal X-ray intensity data were collected at room temperature from a carefully selected, exceptionally large twin (experimental conditions and other details are given in Table 3). A very long detector-crystal-distance (50 mm) was chosen in order to minimise overlap of the reflections from the two twin individuals. The data were corrected for Lorentz, polarisation, background and absorption effects, and reduced to structure factors. Systematic extinctions and structure factor statistics unambiguously indicated the centrosymmetric space group

*P*2₁/*n* (refined unit-cell parameters: *a* = 9.777(3), *b* = 7.358(2), *c* = 17.830(5) Å, β = 92.19(4)°, *V* = 1281.7(6) Å³). The structure was solved by direct methods and refined in *P*2₁/*n* using SHELXS97 and SHELXL97, respectively (Sheldrick, 1997a,b). A sound structure model resulted, but with a large *R*(*F*)-value (~20%) caused by the effects of twinning. A subsequent omission of about 210 reflections which were most strongly affected by the twinning (reflection overlap leading to *F*_{obs} considerably larger than *F*_{calc}) allowed anisotropic refinement of all non-oxygen atoms and reduced *R*(*F*) to 13.3%. As expected, it was impossible to locate H atoms. Since anisotropic refinement of the O atoms resulted in an only very small improvement of the *R*-values, the isotropic description was retained (furthermore, three of the 15 O atoms became 'non-positive definite' during the anisotropic refinement). The final positional and displacement parameters are given in Table 4, and selected bond lengths and angles, calculated bond-valence sums for all atoms, and possible hydrogen bonds are listed in Table 5. A list of observed and calculated structure factors can be obtained from one of the authors (U.K.).

Table 4. Fractional atomic coordinates and displacement parameters (in Å²) for allanpringite.

Atom	<i>x</i>	<i>y</i>	<i>z</i>	<i>U</i> _{eq} / <i>U</i> _{iso}
Fe1*	0.27493(18)	0.6185(2)	0.24870(9)	0.0171(7)
Fe2*	0.74539(17)	0.6422(2)	0.48712(9)	0.0158(7)
Fe3*	0.75612(18)	0.1425(2)	0.48182(10)	0.0173(7)
P1	0.4372(3)	0.6104(4)	0.41119(16)	0.0177(8)
P2	1.0548(3)	0.0969(4)	0.40389(16)	0.0186(8)
O1	0.5892(9)	0.5640(11)	0.4167(4)	0.0214(18)
O2	0.3540(8)	0.4376(10)	0.4233(4)	0.0175(16)
O3	0.4036(9)	0.7604(11)	0.4680(4)	0.0235(19)
O4	0.4020(9)	0.6856(13)	0.3314(5)	0.028(2)
O5	1.0958(8)	0.2626(12)	0.4496(4)	0.0232(18)
O6	1.0789(10)	0.1253(13)	0.3213(6)	0.035(2)
O7	1.1326(8)	-0.0757(11)	0.4270(4)	0.0195(17)
O8	0.9017(8)	0.0651(11)	0.4120(4)	0.0187(17)
Oh9	0.2100(10)	0.8627(12)	0.2254(5)	0.030(2)
Ow10	0.1230(10)	0.5470(14)	0.1677(5)	0.036(2)
Ow11	0.1124(12)	0.6196(15)	0.3313(6)	0.046(3)
Oh12	0.8304(9)	0.3953(11)	0.4809(4)	0.0221(18)
Oh13	0.6734(9)	0.8950(11)	0.4823(5)	0.0257(19)
Ow14	0.8481(9)	0.7077(12)	0.3886(5)	0.0260(19)
Ow15	0.6400(9)	0.2078(12)	0.3796(5)	0.028(2)
Ow16a**	0.811(2)	0.238(4)	0.2513(12)	0.050(6)
Ow16b**	0.775(3)	0.114(4)	0.2496(14)	0.059(7)

Note: $U_{eq} = (1/3)\sum_i U_{ij} a_i^* a_j^* \mathbf{a}_i \cdot \mathbf{a}_j$ (Fischer & Tillmanns, 1988).

* Refined occupancies: Fe1 = Fe_{0.92(2)}Al_{0.08(2)}; Fe2 = Fe_{0.91(2)}Al_{0.09(2)}; Fe3 =

Fe_{0.92(2)}Al_{0.08(2)}

** Split site (see text).

Atom	<i>U</i> ₁₁	<i>U</i> ₂₂	<i>U</i> ₃₃	<i>U</i> ₂₃	<i>U</i> ₁₃	<i>U</i> ₁₂
Fe1	0.0184(11)	0.0090(10)	0.0238(11)	-0.0001(6)	-0.0013(7)	0.0015(7)
Fe2	0.0162(10)	0.0080(9)	0.0231(11)	0.0001(6)	-0.0003(7)	0.0006(6)
Fe3	0.0176(11)	0.0077(9)	0.0265(11)	-0.0009(6)	0.0015(7)	-0.0006(6)
P1	0.0173(15)	0.0138(14)	0.0220(15)	0.0003(10)	0.0001(11)	-0.0006(12)
P2	0.0198(16)	0.0127(14)	0.0232(16)	0.0014(11)	0.0012(12)	0.0026(12)

Description of the crystal structure and relation to wavellite

The crystal structure of allanpringite, ideally Fe₃(PO₄)₂(OH)₃·5H₂O, is a monoclinically distorted, pseudo-orthorhombic variant of the orthorhombic structure of its Al-analogue wavellite, Al₃(PO₄)₂(OH,F)₃·5H₂O (Fig. 2, Table 6). The relations between the axial orientations are as follows (ap = allanpringite): $a_{ap} \sim a_{wav}$, $b_{ap} \sim c_{wav}$, $c_{ap} = b_{wav}$. The space group of allanpringite (*P2₁/n*) is a subgroup of the space group of the wavellite aristotype (*Pcmm*; standard setting: *Pnma*). Crystals of allanpringite and wavellite are both elongated along the short ~ 7 Å axis, parallel to which the structure contains infinite octahedral chains (see below).

The crystal structure of allanpringite is, on account of its close relation to wavellite, also related to those of kingite, Al₃(PO₄)₂(F,OH)₂·8(H₂O,OH) (Wallwork *et al.*, 2003, 2004) and mitryaevaite, Al₅(PO₄)₂[(P,S)O₃(OH,O)]₂F₂(OH)₂(H₂O)₈·6.48H₂O (Cahill *et al.*, 2001).

The asymmetric unit of the new mineral contains three Fe, two P, 16 O and 13 H atoms. The labels for the atoms in

the refined model were chosen to be equivalent to the labeling in wavellite, as far as possible. A refinement of the occupancies of the Fe sites indicated that each of them are partially replaced by Al atoms, with refined Fe:Al ratios between 91(2):9(2) and 92(2):8(2) (Table 4). However, considering the effects of the twinning, the true ratios might somewhat differ from these refined values.

The crystal structure is based upon chains of corner-sharing, distorted Fe(O,OH,H₂O)₆ octahedra parallel to the *b* axis (Figs. 2a; 3a,c). These chains are linked together by PO₄ tetrahedra via common oxygen atoms. The resulting channels, also parallel to the *b* axis, host a positionally split water molecule (Ow16a, Ow16b; Ow16a–Ow16b = 0.98(3) Å). The position of the equivalent Ow atom in the corresponding channels of wavellite (Araki & Zoltai, 1968) is also split, with a similar distance between the two half-occupied sites (0.90 Å). The average Fe–O distances are fairly similar (Fe1: 2.014 Å, Fe2: 2.018 Å, Fe3: 2.021 Å) and prove, along with calculated bond-valence sums (Table 5), that all Fe atoms are in the trivalent state. All Fe(O,OH,H₂O)₆ octahedra are distorted, with intra-octahedral angles deviating up to 14.7°

Table 5. Selected bond distances (Å) and bond angles (°) for the coordination polyhedra in allanpringite, and calculated bond valences.

Fe1–O6	1.933(10)	0.625	Fe3–O3	1.963(9)	0.576
–Oh9	1.942(9)	0.610	–O7	1.983(8)	0.546
–Oh9	1.945(9)	0.605	–Oh13	1.993(9)	0.531
–O4	1.955(9)	0.584	–Oh12	1.997(8)	0.526
–Ow10	2.099(10)	0.399	–O8	2.008(8)	0.510
–Ow11	2.207(12)	<u>0.298</u>	–Ow15	2.164(9)	<u>0.335</u>
<Fe1–O>	2.014	3.13 v.u.	<Fe3–O>	2.018	3.02 v.u.
Fe2–O2	1.989(8)	0.537	Ow16a–Ow16b	0.98(3)	
–Oh13	1.989(9)	0.537			
–Oh12	2.003(8)	0.517			
–O5	2.010(8)	0.507			
–O1	2.024(8)	0.489			
–Ow14	2.113(8)	<u>0.384</u>			
<Fe2–O>	2.021	2.97 v.u.			
P1–O1	1.524(9)	1.241	P2–O5	1.512(9)	1.282
–O2	1.529(8)	1.225	–O6	1.515(10)	1.272
–O3	1.543(8)	1.179	–O7	1.528(8)	1.228
–O4	1.553(9)	<u>1.148</u>	–O8	1.528(8)	<u>1.228</u>
<P1–O>	1.537	4.79 v.u.	<P2–O>	1.521	5.01 v.u.
O1–P1–O2	109.1(5)		O5–P2–O6	111.4(5)	
O1–P1–O3	110.5(5)		O5–P2–O8	108.2(5)	
O2–P1–O3	112.0(5)		O6–P2–O8	107.6(5)	
O1–P1–O4	108.7(5)		O5–P2–O7	113.9(5)	
O2–P1–O4	109.0(5)		O6–P2–O7	106.4(5)	
O3–P1–O4	107.5(5)		O8–P2–O7	109.0(5)	
<O–P1–O>	109.5		<O–P2–O>	109.4	

Bond-valence sums (v.u.) for the O atoms O1 – OW16 are as follows: 1.73 (O1); 1.76 (O2); 1.76 (O3); 1.73 (O4); 1.79 (O5); 1.90 (O6); 1.77 (O7); 1.74 (O8); 1.22 (Oh9); 0.40 (Ow10); 0.30 (Ow11); 1.04 (Oh12); 1.07 (Oh13); 0.38 (Ow14); 0.33 (Ow15); 0.00 (Ow16a / Ow16b). *Note:* Bond-valence parameters used are from Brese & O’Keeffe (1991). If the minor Al-for-Fe-substitution on the three Fe sites were taken into account, slightly smaller bond-valence sums for these sites would result.

Possible hydrogen bonds (Å)*

Oh9...O2	2.756	Ow15...Ow16b	2.797
Ow10...Ow15	2.925	Ow15...Ow16a	2.893
Ow10...O7	3.112	Ow16a...Ow15	2.893
Ow11...O7	2.820	Ow16a...Ow14	2.897
Ow11...Ow14	2.888	Ow16a...O6	2.976
Oh12...O5	2.848	Ow16b...Ow14	2.787
Oh13...O3	2.820	Ow16b...Ow15	2.797
Ow14...Ow16b	2.787	Ow16b...O8	3.126
Ow14...Ow11	2.888	Ow16b...O6	3.190
Ow14...Ow16a	2.897		

* Only O...O distances < 3.2 Å are considered.

from ideal angles (the maximum distortion is shown by the Fe1-centred octahedron). The average P–O distances are somewhat different (P1: 1.537 Å, P2: 1.521 Å), but very close to commonly observed values in phosphate minerals (e.g., Huminicki & Hawthorne, 2002). A complex system of medium-strong to weak H bonds reinforces the polyhedral framework; this scheme involves all OH groups and water molecules in the structure (Table 5). The donor-acceptor distances range between 2.756 and about 3.2 Å.

The lower symmetry of allanpringite (monoclinic-pseudo-orthorhombic) as compared to wavellite (orthorhombic) is due to a slight zig-zag-like tilting of the Fe1O₆-based octahedral chains extending along the *b*-axis (corresponding to the *c*-axis of wavellite). This tilting is suitably demonstrated by a comparative view of the polyhedral connectivity along the *a*-axis, i.e. perpendicular to the tilted chains

(Fig. 2). In contrast, in views along *b* (= *c*_{wav}) and *c* (= *b*_{wav}) the crystal structures of allanpringite and wavellite appear nearly identical (Fig. 3). The tilting of the Fe1O₆-based octahedral chain in allanpringite is tentatively explained as follows: the Fe1O₆ octahedron is larger than the corresponding Al1O₆ octahedron in wavellite (as well as also slightly larger than the Fe2O₆ octahedron), and thus a tilting of the chain is necessary in order to accommodate it into the framework. The tilting appears to be mainly responsible for the loss of the orthorhombic symmetry (the angle β deviates by 2.2° from a right angle). As a consequence, the Al2 atom in wavellite is split into two positions in allanpringite (Fe2 and Fe3). Furthermore, the P atom in wavellite has two counterparts in allanpringite (P1 and P2), and several O atom sites are also split due to the symmetry reduction. The persistent twinning by non-merohedry of allanpringite is at-

Table 6. Comparison of allanpringite, wavellite and santabarbarite.

Mineral	Allanpringite	Wavellite	Santabarbarite
Ref.	This work	Araki & Zoltai (1968)*	Pratesi <i>et al.</i> (2003)
Formula	Fe ₃ (PO ₄) ₂ (OH) ₃ ·5H ₂ O	Al ₃ (PO ₄) ₂ (OH,F) ₃ ·5H ₂ O	Fe ₃ (PO ₄) ₂ (OH) ₃ ·5H ₂ O
<i>a</i> (Å)	9.777(3)	9.621	-
<i>b</i> (Å)	7.358(2)	17.363	-
<i>c</i> (Å)	17.830(5)	6.994	-
β (°)	92.19(4)	-	-
<i>V</i> (Å ³)	1281.7(6)	1168.3	-
Symmetry	monoclinic	orthorhombic	amorphous
Space group	<i>P</i> 2 ₁ / <i>n</i>	<i>Pcmm</i>	-
<i>Z</i>	4	4	-
5 strongest lines in the powder pattern	8.90 (100), 3.231 (80), 8.41 (60), 5.870 (50), 3.600 (50)	8.67 (100), 8.42 (100), 3.22 (60), 5.65 (50), 3.42 (42)	amorphous
D(meas.); (calc.)	2.54; 2.58	2.30-2.36; 2.34	2.42; -
Mohs Hardness	~3	3½-4	n.d.
α	1.662(5)	1.518-1.535	
β	1.675(5)	1.524-1.543	n = 1.695
γ	1.747(5)	1.544-1.561	
Birefringence	0.085	0.026	0.0
Opt. character	2(+) (not observable; inferred from indices)	2(+)	isotropic
2 <i>V</i> (meas.); (calc.)	not observable; 48°	~50-72°; ~79°	-; -
Dispersion	none observable	r > v, weak	-
Orientation	XYZ = **b (pseudo-orthorhombic)	XYZ = bac	-
Elongation	pos.	pos.	-
X (colour)	colourless	colourless to greenish	
Y (colour)	colourless	colourless	
Z (colour)	dark yellow	colourless to yellowish	
Absorption	Z >> X-Y	X > Z	-
Megascopic colour	pale brownish-yellow	colourless, white; also greenish, yellowish, brownish	brown to light brown
Tenacity	brittle	brittle	brittle
Streak	white with pale yellowish tint	colourless	yellowish amber
Habit	acicular [010]	acicular to prismatic [001], striated // [001]	massive (as pseudomorphs)**
Twinning	always, // to [010]	none	-
Cleavage	one perfect cleavage // to elongation (probably {101} by analogy with wavellite); {010} good	{110} perfect, {101} good, {010} distinct	n.d.
Fracture	uneven	subconchoidal to uneven	conchoidal

* supplemented with data from Anthony *et al.* (2000).

** Pseudomorphs formed by *in-situ* oxidation of vivianite (alteration sequence: vivianite-metavivianite-santabarbarite).

tributed to its monoclinic-pseudo-orthorhombic symmetry. Although the twin plane could not be unambiguously identified, it is assumed to be (100), i.e., the twin plane corresponds to the symmetry plane lost due to the monoclinic distortion of the framework. It is worth noting that no twinning has ever been reported for wavellite.

The discovery of allanpringite leads to the question whether there exists a solid solution series with its Al-analogue wavellite in nature. A large number of chemical analyses of wavellite have been reported but all show only rather minor Fe contents (≤3 wt. % Fe₂O₃) and, frequently, a minor F-for-OH substitution. The apparent non-existence of intermediate wavellite-allanpringite solid solution members in natural environments may indicate a solid solution gap between both species. Nonetheless, a hypothetical Fe-rich va-

riety of wavellite may have the same (monoclinic) symmetry as allanpringite. The extreme rarity of allanpringite in nature also suggests that the mineral has either a very narrow stability field or is a metastable phase. Laboratory preparation of synthetic material may be necessary to answer these questions.

Relation between allanpringite and santabarbarite

Allanpringite has (nearly) the same chemical formula as the amorphous species santabarbarite (Pratesi *et al.*, 2003) and may be considered as a polymorph of santabarbarite. However, the latter forms exclusively on *in-situ* oxidative alteration of vivianite, Fe²⁺₃(PO₄)₂·8H₂O, with triclinic metavi-

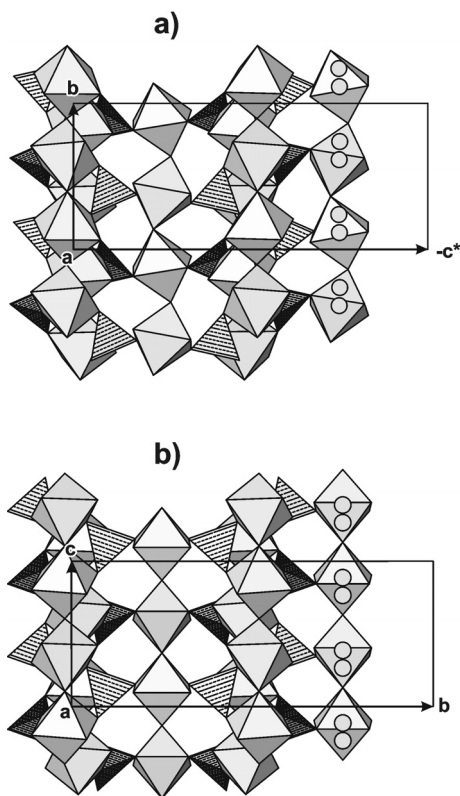


Fig. 2. Comparative view of the crystal structures of allanpringite (a) and wavellite (b) in a view along the respective a -axes. $M(\text{O},\text{OH},\text{H}_2\text{O})_6$ ($M = \text{Fe}, \text{Al}$) octahedra are unmarked, PO_4 tetrahedra are marked with dashed lines, and the split water site (Ow16 in allanpringite) is shown as small spheres. All drawings were done with ATOMS (Shape Software, 1999).

vianite, $\text{Fe}^{2+}_{3-x}\text{Fe}^{3+}_x(\text{PO}_4)_2(\text{OH})_x \cdot (8-x)\text{H}_2\text{O}$, as an intermediate phase in the alteration process (Pratesi *et al.*, 2003). Thus, the genesis is completely different from that of allanpringite which crystallises in a secondary phosphate assemblage. Physical properties and spectroscopic data of santabarbaraite are completely different from those of allanpringite. Table 6 provides a comparison of allanpringite, wavellite and santabarbaraite.

Raman spectroscopy

Laser-Raman spectra of twinned crystals of allanpringite were recorded in the range from 4000 to 200 cm^{-1} with a Renishaw M1000 MicroRaman Imaging System using a laser wavelength of 488 nm and excitation through a Leica DMLM optical microscope (unpolarised laser light, 180° backscatter mode, spectral resolution $\pm 2 \text{ cm}^{-1}$, minimum lateral resolution $\sim 2 \mu\text{m}$, random sample orientation). The crystals were stable under the laser beam and the spectra are of good quality. Two representative spectra (Fig. 4) show bands (strong ones are underlined; sh = shoulder) due to OH stretching vibrations (at ~ 3567 , 3412, ~ 3197 , ~ 3060 to ~ 3052 sh cm^{-1}), H-O-H bending vibrations of water molecules ($\sim 1625 \text{ cm}^{-1}$), vibrations of the PO_4 tetrahedra (ν_1 and ν_3 : ~ 1100 sh, 1060, 1023, 1009, 987 cm^{-1}) and a region below 600 cm^{-1} with overlapped bands due to the ν_4 (and ν_2)

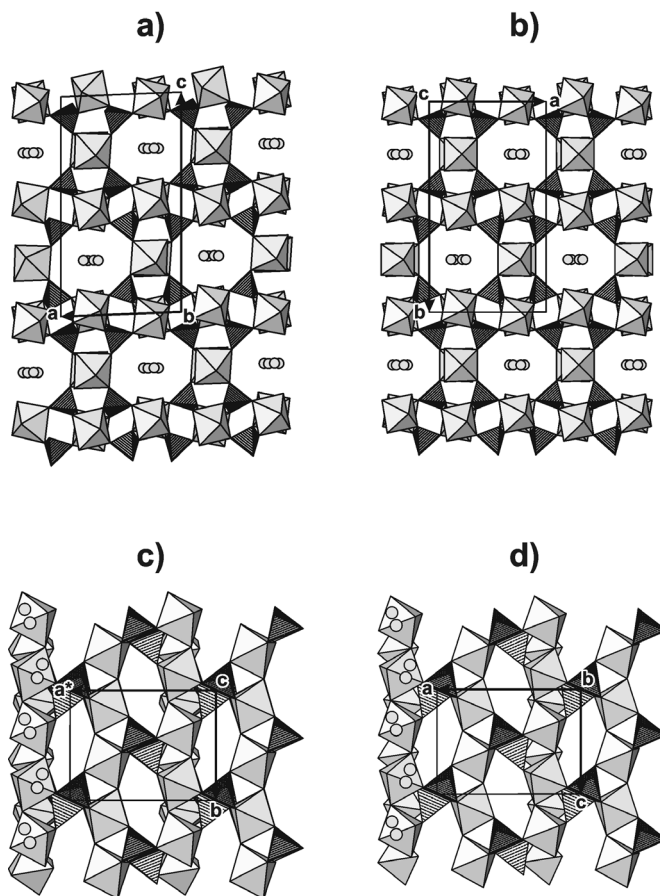


Fig. 3. Comparison between the crystal structures of allanpringite (a,c) and wavellite (b,d) in two corresponding views along the b_{ap} (a) and c_{ap} (c) axes (see text for discussion). Compare Fig. 2.

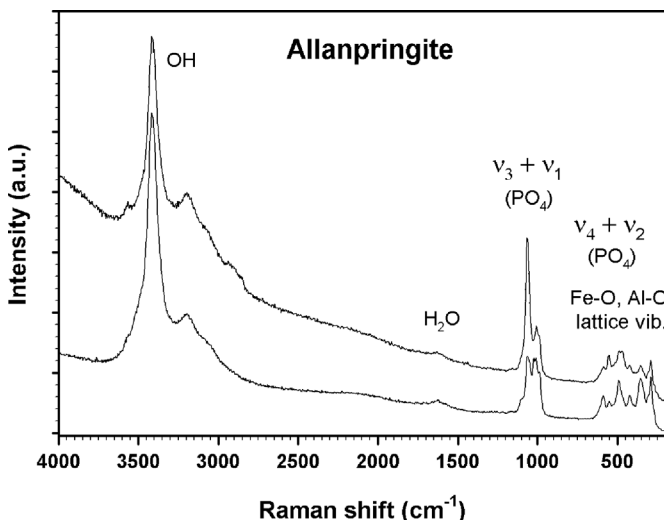


Fig. 4. Two representative laser-Raman spectra of twinned crystals of allanpringite (see text for band positions and tentative interpretation).

vibrations of the PO_4 tetrahedra, vibrations of the $\text{Fe}(\text{O},\text{OH},\text{H}_2\text{O})_6$ octahedra, and lattice modes (590, 555, 516, 491, 470, 424, 355, ~ 309 , 292 cm^{-1}). The positions of the OH bands agree well with those expected from $\text{O}\cdots\text{O}$

donor-acceptor distances (see correlation curve established by Libowitzky, 1999).

Acknowledgements: Mr. Michael Legner is thanked for kindly providing the studied samples and some helpful information. The article was improved by constructive comments of two anonymous referees. Financial support by the Austrian Science Foundation (FWF) (Grant P15220-N06) is gratefully acknowledged.

References

- Anthony, J.W., Bideaux, R.A., Bladh, K.W., Nichols, M.C. (2000): Handbook of Mineralogy. Vol. IV: Arsenates, phosphates, vanadates. Mineral Data Publishing, Tucson, Arizona, USA, 680 pp.
- Araki, T. & Zoltai, T. (1968): The crystal structure of wavellite. *Z. Kristallogr.*, **127**, 21–33.
- Blaß, G. (2002): Eine neue Phosphatmineralien-Paragenese von der Grube Mark bei Essershausen, mittleres Lahnggebiet, Taunus. *Mineralien-Welt*, **13** (6), 18–43. (in German).
- Brese, N.E. & O’Keeffe, M. (1991): Bond-valence parameters for solids. *Acta Crystallogr.*, **B47**, 192–197.
- Cahill, C.L., Krivovichev, S.V., Burns, P.C., Bekenova, G.K., Shabanova, T.A. (2001): The crystal structure of mitryaevaite, $\text{Al}_5(\text{PO}_4)_2[(\text{P,S})\text{O}_3(\text{OH},\text{O})]_2\text{F}_2(\text{OH})_2(\text{H}_2\text{O})_8 \cdot 6.48\text{H}_2\text{O}$, determined from a microcrystal using synchrotron radiation. *Can. Mineral.*, **39**, 179–186.
- Fischer, R.X. & Tillmanns, E. (1988): The equivalent isotropic displacement factor. *Acta Crystallogr.*, **C 44**, 775–776.
- Huminicki, D.M.C. & Hawthorne, F.C. (2002): The crystal chemistry of the phosphate minerals. in “Phosphates – geochemical, geobiological, and materials importance”, *Reviews in Mineralogy and Geochemistry*, Vol. **48**, Kohn, M.J., Rakovan, J. & Hughes, J.M., eds. Mineral. Soc. of Am., Washington, D.C. and Geochem. Soc., St. Louis, MO, USA, 123–253.
- Kolitsch, U. (1999): Evidence for the identity of meurigite and phosphofibrite by transmission electron microscopy and X-ray powder diffraction. *Eur. J. Mineral.*, **11**, Beih. No. 1, 132 (abstr.).
- (2001): The atomic arrangement of the fibrous iron phosphate ‘laubmannite’ (as defined by Moore, 1970). *Eur. J. Mineral.*, **13**, Beih. No. 1, 99 (abstr.).
- (2004): The crystal structures of kidwellite and ‘laubmannite’, two complex fibrous iron phosphates. *Mineral. Mag.*, **68**, 147–165.
- Kolitsch, U., Bernhardt, H.-J., Blaß, G. (2004): $\text{Fe}_3(\text{PO}_4)_2(\text{OH})_3 \cdot 5\text{H}_2\text{O}$, a new monoclinic ferric iron phosphate mineral from Germany: crystal structure, single-crystal Raman spectra and close relation to wavellite. *Mitt. Österr. Mineral. Ges.*, **149**, 50.
- Libowitzky, E. (1999): Correlation of O-H stretching frequencies and O-H...O hydrogen bond lengths in minerals. *Monatsh. Chem.*, **130**, 1047–1059.
- Otwinowski, Z. & Minor, W. (1997): Processing of X-ray diffraction data collected in oscillation mode. *Methods Enzymol.*, **276**, 307–326.
- Otwinowski, Z., Borek, D., Majewski, W., Minor, W. (2003): Multi-parametric scaling of diffraction intensities. *Acta Crystallogr.*, **A59**, 228–234.
- Pratesi, G., Cipriani, C., Giuli, G., Birch, W.D. (2003): Santabarbarite: A new amorphous phosphate mineral. *Eur. J. Mineral.*, **15**, 185–192.
- Shape Software (1999): ATOMS for Windows and Macintosh V5.0.4. Kingsport, TN 37663, U.S.A.
- Sheldrick, G.M. (1997a): SHELXS-97, a program for the solution of crystal structures. University of Göttingen, Germany.
- , –, – (1997b): SHELXL-97, a program for crystal structure refinement. University of Göttingen, Germany.
- Wallwork, K.S., Pring, A., Taylor, M.R., Hunter, B.A. (2003): A model for the structure of the hydrated aluminum phosphate, kingite determined by ab initio powder diffraction methods. *Am. Mineral.*, **88**, 235–239.
- , –, – (2004): The network of hydrogen bonding in kingite, as revealed by a neutron-diffraction investigation of its deuterated analogue, $\text{Al}_3(\text{PO}_4)_2\text{F}_3 \cdot 7\text{D}_2\text{O}$. *Can. Mineral.*, **42**, 135–141.

Received 15 July 2005

Modified version received 6 April 2006

Accepted 15 September 2006